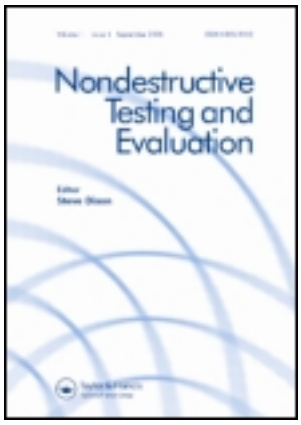

Nondestructive Testing and Evaluation
Publication details, including instructions for authors and subscription information:
http://www.tandfonline.com/loi/gnte20

Advanced automated optical inspection system for fishtail collapse of microrouter

Der-Baau Perng [a] & Yen-Chung Chen [a]
[a] Department of Industrial Engineering and Management , National Chiao Tung University , HsinChu, Taiwan, 30010, ROC
Published online: 23 Oct 2008.

To cite this article: Der-Baau Perng & Yen-Chung Chen (2008) Advanced automated optical inspection system for fishtail collapse of microrouter, Nondestructive Testing and Evaluation, 23:4, 257-272, DOI: 10.1080/10589750802200756

To link to this article: http://dx.doi.org/10.1080/10589750802200756

Nondestructive Testing and Evaluation,
Vol. 23, No. 4, December 2008, 257–272

Taylor & Francis
Taylor & Francis Group

Advanced automated optical inspection system for fishtail collapse of microrouter

Der-Baau Perng* and Yen-Chung Chen

Department of Industrial Engineering and Management, National Chiao Tung University, HsinChu, Taiwan 30010, ROC

(*Received 24 October 2007; final version received 14 May 2008*)

In this paper, an innovative automated optical inspection (AOI) system is proposed to detect fishtail collapse of various fishtail images. Up to the present, there is no report on the inspection of fishtail collapse by using an AOI system. The proposed AOI system is the first system that can inspect the fishtail collapse of microrouter. The fishtail image of the microrouter was extracted first by a newly developed lighting device. We use the end gash to identify one of the blades as the reference blade, in order to provide an orientation-invariant method to solve the fishtail image rotation problem. Three invariant features of the blade are used as indicators of quality control. The blade with collapse, whose area is as small as 0.02 mm × 0.02 mm, could be identified based on the constructed quality control charts. Twenty-five fishtail images are used to validate the proposed AOI system. The successful detection rate of the implemented AOI system is up to 99.2%, and it demonstrates that this system detects the collapse accurately and robustly.

Keywords: microrouter; fishtail; automated optical inspection; collapse

1. Introduction

Printed circuit board (PCB) is an important component of most electronic products. Its quality affects the stability of the electronic product. One of the significant factors that affect the PCB quality is the PCB tool. A diamond-cut microrouter (router) is a PCB tool that is used for chip removal and PCB cutting. The diameter of the router is as small as 0.6 mm, and it has diamond-cut and fishtail geometry. Figure 1 shows the side view of the router, where the fishtail is indicated by the dotted rectangle. The fishtail is mainly used to drill holes in the PCB that is helpful in cutting the PCB afterward. Hence, it is very important to ensure that the fishtail is defect free.

So far, in router manufacturing companies, fishtail defects have been inspected by human inspectors using electronic microscopes. However, the human inspectors have a disadvantage – they are prone to weariness caused by long-term working. So, in this paper, we propose an automated optical inspection (AOI) system to inspect fishtail defects. However, there is no report on the inspection of router defects by using the AOI system except some related studies on the inspection of a microdrill, which is used to drill holes in the PCB and shown in Figure 2. Tien *et al.* [6] have proposed a position- and orientation-invariant method to inspect microdrill defects. Perng *et al.* [4] have proposed a machine vision system that uses a position-invariant method to measure the diameter and length of the microdrill automatically.

Figure 3 shows the fishtail image captured by the proposed AOI system. There are different types of routers, and each router has a distinct fishtail pattern. The fishtail pattern is generated by

* Corresponding author. Email: perng@cc.nctu.edu.tw

ISSN 1058-9759 print/ISSN 1477-2671 online

DOI: 10.1080/10589750802200756
http://www.informaworld.com

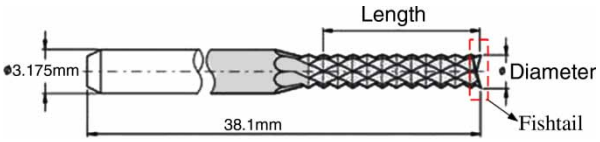

Figure 1. Side view of a router with fishtail.

three machining procedures: right flute cutting, left flute cutting, and fishtail cutting. Different fishtail patterns are created by changing a machining parameter of these machining procedures. Figure 4 shows three different fishtail patterns corresponding to different machining parameters. Hence, routers which are produced by the same machine with identical parameters in a particular batch are used for fishtail collapse inspection in this study. Connected object labelling [5] scans the image and groups its pixels into objects based on pixel connectivity, then extracts fishtail pattern from these objects. The features of the fishtail pattern, such as area, boundary length, curvature, intensity, and statistical moments [2], can be extracted by image processing methods. Then, these features can be used to detect the collapsed blade of various fishtail patterns by using the proposed AOI system.

This paper is organised as follows. The hardware system and software algorithms of the proposed AOI system are described in Section 2. The experimental results for two different fishtail patterns are discussed in Section 3. The conclusions and some suggestions are provided in Section 4.

2. AOI system for fishtail collapse inspection

The fishtail consists of two inclined planes that have opposite angles as shown in Figure 5. The angle formed by the two inclined planes is a parameter used in the fishtail cutting procedure. That is, the geometric pattern of the fishtail is affected by the two inclined planes. The hardware architecture of the proposed AOI system for fishtail pattern extraction is shown in Figure 6. It consists of a fixture, reflective light emitting diode (LED) ring illuminator, charge-coupled device (CCD) camera, and a horizontally movable stage. The fixture is used to hold the router.

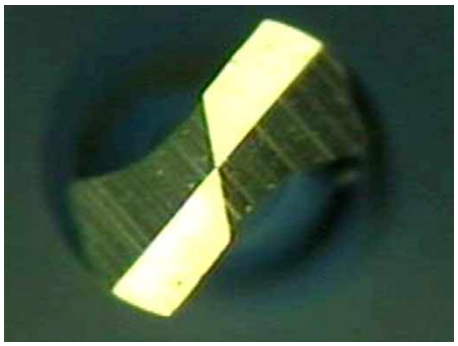

Figure 2. Image of normal microdrill.

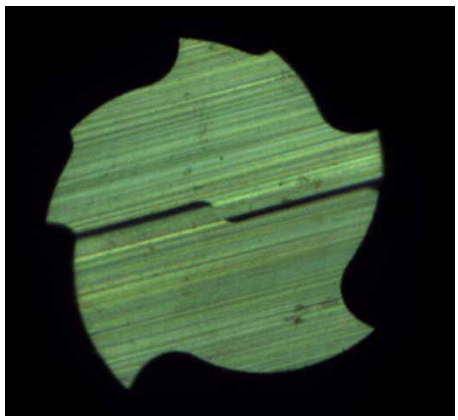

Figure 3. Front view image of a fishtail captured by the proposed AOI system.

The reflective LED ring illuminator is used to illuminate the two inclined planes. The movable stage is used to move CCD to capture clear images.

In general, faultless routers from the same batch have similar fishtail patterns and a fishtail pattern usually consists of more than one blade. Since the router is mounted arbitrarily on the fixture, the orientation of each mounted fishtail will be varied. Two samples of fishtail patterns from a batch are shown in Figure 7(a) and (b), in which each blade is illustrated to be bounded by a pseudo-rectangle. The examination of the fishtail implies the inspection of its blades for defects. Figure 8 shows a fishtail image in which there is a collapse on the blade. The fishtail collapse inspection includes the training and testing phases. The purpose of training phase is to determine the upper control limits (UCLs) and lower control limits (LCLs) which will be utilised to check if the blades of fishtails have defects in the testing phase. The flowchart of the proposed fishtail collapse inspection system is shown in Figure 9.

2.1 Fishtail pattern extraction

To extract the fishtail pattern from the captured image for easy inspection, the fishtail in the image is illuminated by the reflective LED ring illuminator in contrast with the background, as shown in Figure 10. Due to the high contrast of the captured image, we can determine the fishtail by thresholding at a controllable intensity level. The threshold value could be determined according to the histogram of the captured image as shown in Figure 11. The lower peak on the right side is formed by the fishtail pixels, while the higher peak on the left side is constituted by pixels of the dark background. It is a typical two dominant modes distribution. To separate the two groups of pixels, a suggested threshold can be set by averaging the two peak values. Each of the two fishtail images in Figure 10 was binarised under the suggested threshold as shown in Figure 12.

2.2 Fishtail centre identification

Once a fishtail pattern is obtained, the boundary of the fishtail pattern is used for fishtail pattern description. The boundary includes the shape features as well as information on the collapse of the blade of fishtail. Because the centre (machining centre) of the fishtail is orientation invariant and not affected by blade collapse, the centre of the fishtail is helpful in describing the boundary of the fishtail. Fishtail centre is also used as a reference for blade identification. For each original fishtail, there are two end gashes as shown in Figure 13. We use the two end gashes to identify the centre of the fishtail. First, we perform a closing operation of morphology [5] on the image to

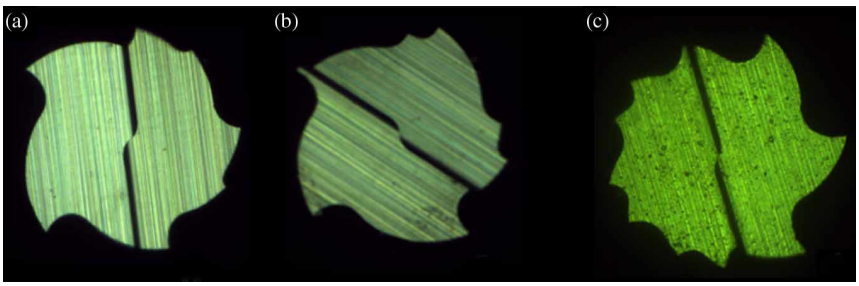

Figure 4. Images of three different fishtail patterns; patterns A and B have five right flutes, while pattern C has seven right flutes.

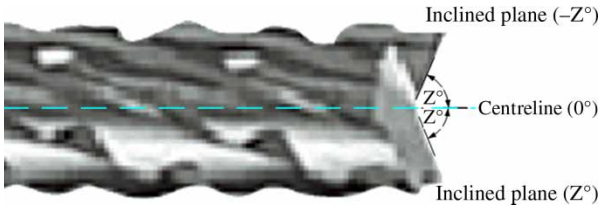

Figure 5. Side view image of a fishtail.

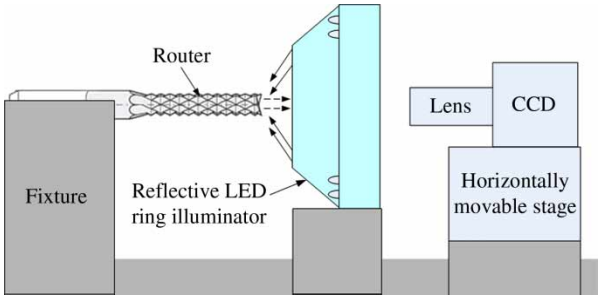

Figure 6. Schematic of the proposed AOI hardware for fishtail pattern extraction and inspection.

fill in the two end gashes, as in the filled fishtail shown in Figure 14. Second, different parts between the original fishtail and the filled fishtail were calculated and grouped into a set. Third, the connected object labelling method [5] is used to select the two largest areas, which are the end gashes $T1$ and $T2$, from the set of different parts, as shown in Figure 15. Fourth, the minimum distance between two end gashes is calculated. We assume that the set of boundary pixels of $T1$ and $T2$ are $\{T1\}$ and $\{T2\}$, respectively. Let a, with coordinate (X_a, Y_a), be

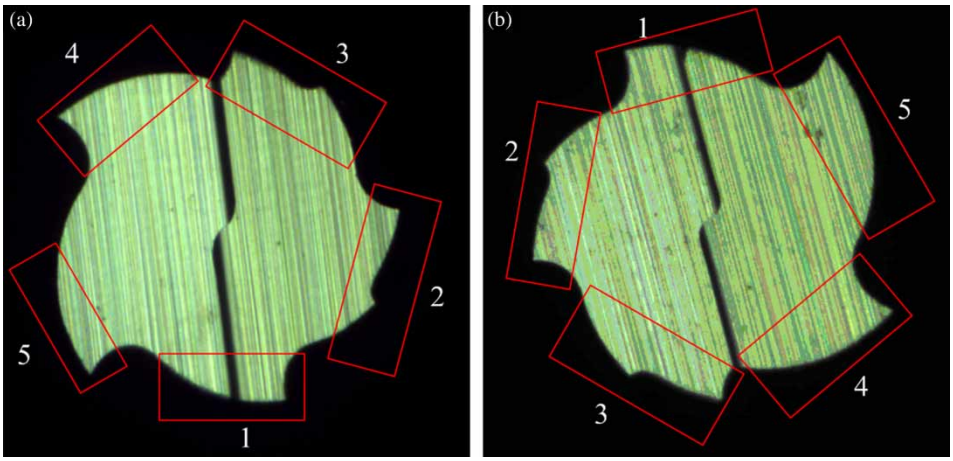

Figure 7. (a) and (b) Sample images of different fishtail patterns. There are five blades in each fishtail. Each blade of a fishtail is bounded by a pseudo-rectangle and is assigned a unique blade number.

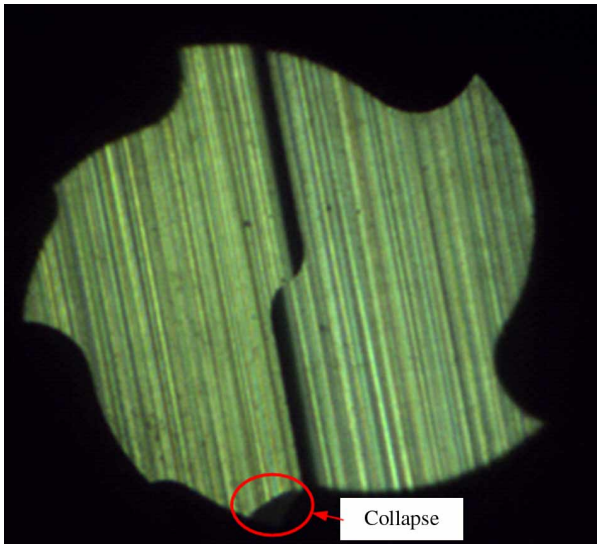

Figure 8. Image of a collapsed blade of a fishtail.

a boundary pixel in $\{T1\}$ and b, with coordinate (X_b, Y_b), be a boundary pixel in $\{T2\}$. A pair of boundary pixels $\{a, b\}$ is determined by equations (1) and (2). D_{ab} is the minimum distance between any pair of pixels of the two sets $\{T1\}$ and $\{T2\}$

$$D_{ab} = \sqrt{(X_a - X_b)^2 + (Y_a - Y_b)^2}, \tag{1}$$

and

$$D_{ab} = \text{Min}\{(D_{ab})|a \subset \{T1\}, \quad b \subset \{T2\}\}, \tag{2}$$

where (X_a, Y_a) and (X_b, Y_b) are the coordinates of the boundary pixels a and b, respectively.

Finally, the centre point C of the line segment $\overline{ab}$ is found to coincide with the centre of the fishtail, as shown in Figure 15. Hence, the coordinate of fishtail centre is $((X_a + X_b)/2, (Y_a + Y_b)/2)$.

2.3 Boundary edge extraction and coordinate transformation

After the determination of the centre of the fishtail, the boundary edge of the fishtail can be derived as a centroidal profile [1]. Let L_c denote a line that passes through the centre of fishtail C and is parallel to the X-axis. Let $\{I\}$ denote a set of intersection pixels formed by the boundary pixels of the filled fishtail and L_c. Assume that the boundary pixels of the filled fishtail in Figure 16 are $\{P_0, P_1, \ldots, P_{n-1}, P_n = P_0\}$. P_0 is the boundary pixel that has the largest value of the X-coordinate in $\{I\}$. The set of Euclidean distances between C and each of the boundary pixels are $\{D_{cp}\} = \{D_{cp0}, D_{cp1}, \ldots, D_{cpn-1}\}$, as shown in Figure 16. Using the centre of the fishtail as a reference centre, we can plot each of the boundary pixels in a graph in the polar coordinate system (γ, θ), as shown in Figure 17.

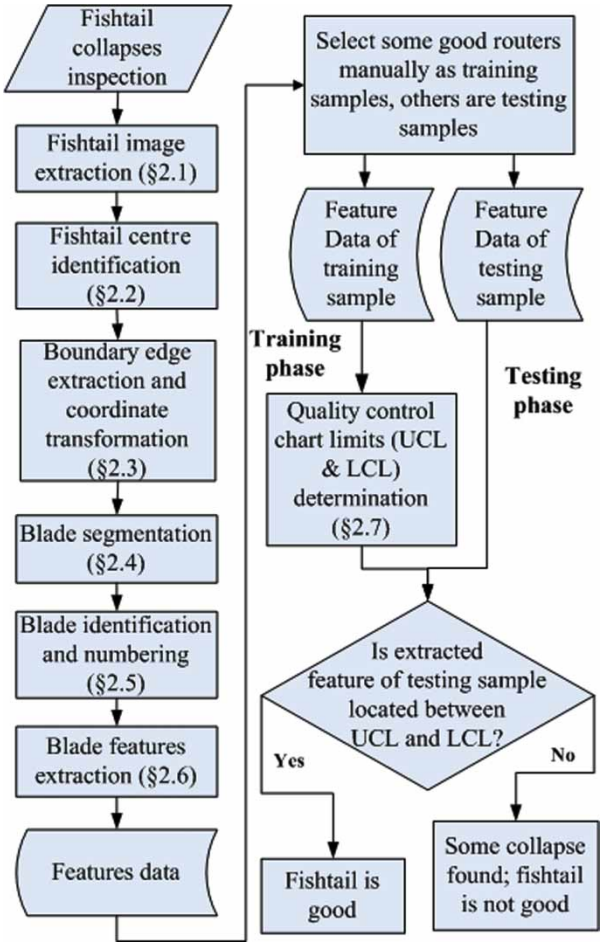

Figure 9. Flowchart of the proposed fishtail collapse inspection method.

2.4 Blade segmentation

A fishtail is generated by three cutting procedures using grinding wheels. Figure 18 shows the centroidal profile of a fishtail with five blades. For a fishtail with five blades, five valleys are generated by the right flute cutting procedure. The interval between two neighbouring right flute

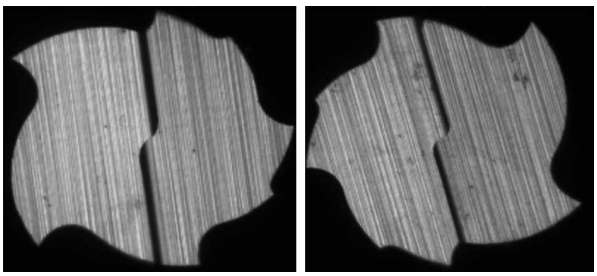

Figure 10. Fishtail part of the captured image illuminated by the reflective LED ring illuminator.

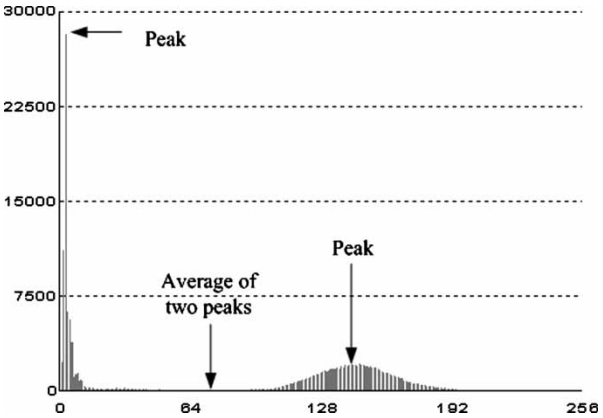

Figure 11. Histogram of the captured image.

Figure 12. Binarised fishtail image under the suggested threshold.

valleys is approximately 72° (=360°/5). Each right flute valley has a corresponding boundary pixel of the fishtail. The valley helps in segmenting an individual blade from the fishtail. We can estimate V_1, which has a global minimum value of $\{D_{cp}\}$. V_1 has corresponding coordinates in (γ, θ). It can be identified as the first right flute valley. Then, we proceed to find out the other local minima of $\{D_{cp}\}$ in about every specific angle degree starting from V_1. These local minima could be identified as other right flute valleys. The right flute valleys obtained in this way are grouped into a valley set $\{V\}$. In the case of a fishtail with five right flutes, the position where a local minimum in $\{D_{cp}\}$ can be found will locate at about every angle degree of 72° starting from V_1 as shown in Figure 18.

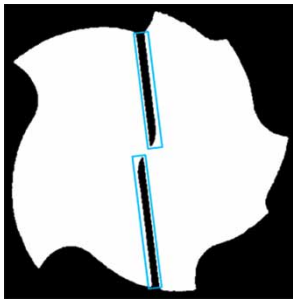

Figure 13. Two end gashes of an original fishtail.

Figure 14. Filled fishtail (from Figure 13).

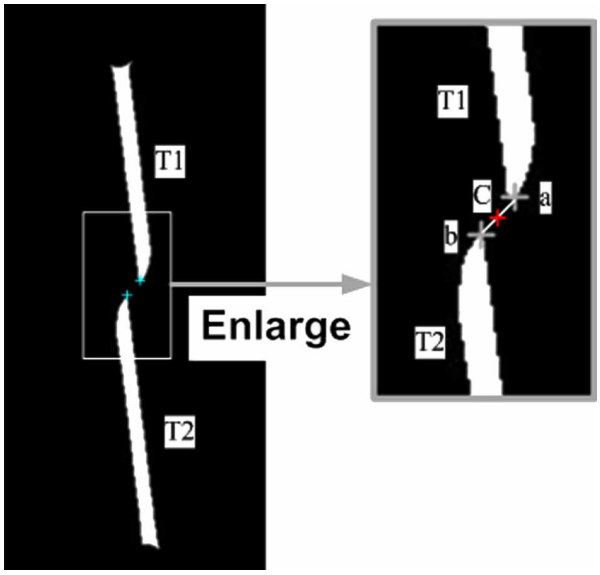

Figure 15. Two extracted end gashes and the determined centre of the fishtail.

2.5 *Blade identification and numbering*

Each right flute valley has corresponding boundary pixels of the fishtail in the (X, Y) coordinate system as the initial pixel of the blade. Any two neighbouring right flute valleys can be connected by a line segment such as $\overline{V_1V_2}$, $\overline{V_2V_3}$, $\ldots$, $\overline{V_5V_1}$ as shown in Figure 19. A blade of a fishtail can be defined as a set of boundary pixels from a right flute valley V_i along the successive boundary pixels of the fishtail pattern to the next right flute valley V_{i+1} and the line segment $\overline{V_iV_{i+1}}$. All the blades can then be identified and segmented from the fishtail as shown in Figure 18. Owing to the various

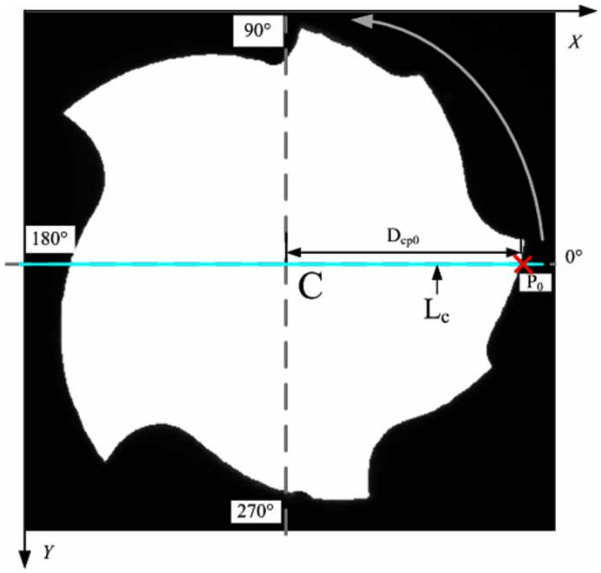

Figure 16. Illustration of coordinate transformation of the boundary pixels of a fishtail.

Figure 17. Centroidal profile of the boundary pixels of a fishtail with respect to the centre of the fishtail.

orientations, we need to identify one blade of each fishtail as the initial or reference blade. For example, in Figure 7(a) and (b), the blade numbered as '1' is the reference blade and the other blades are numbered successively in the counterclockwise direction. Arbitrary blades that have the same blade number of different fishtails will have similar shape. The end gashes, $T1$ and $T2$, will affect the shape of the blade, as shown by the white dotted line in Figure 19. This property is employed to identify a reference blade. The reference blade helps to define the orientation of the fishtail. We use equation (3) to identify a blade that has a heavy intersection with the end gashes ($T1 \cup T2$) and refer to it as the reference blade. The remaining blades can be identified and numbered successively in the counterclockwise direction as shown in Figure 19(a). Each blade in the different fishtail patterns, patterns B and C in Figure 4, can also be identified by the proposed method as shown in Figure 19(b) and (c).

$$\begin{aligned} \text{Definition of reference blade}: \ & \text{It is a blade with a maximum value in} \\ & \{\text{Area}(\text{Blade}_i) \cap \text{Area}(T1 \cup T2)\}, \text{ where} \\ & i = 1, \ldots, n, \ n = \text{number of right flutes.} \end{aligned} \tag{3}$$

2.6 Feature analysis

After obtaining the information on the shape, position, and assigned number of all the blades, three invariant features of the blade are used to check whether any collapse exists. The invariant features are the area, boundary length, and statistic of the vector angle. If a collapse occurs, then

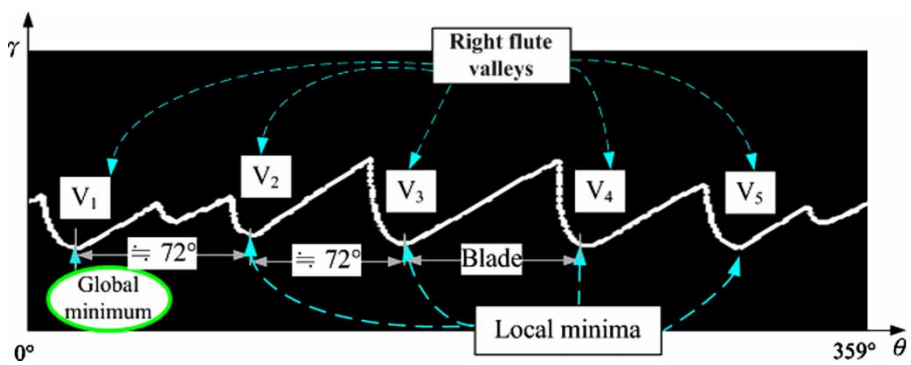

Figure 18. Identification of right flute valleys.

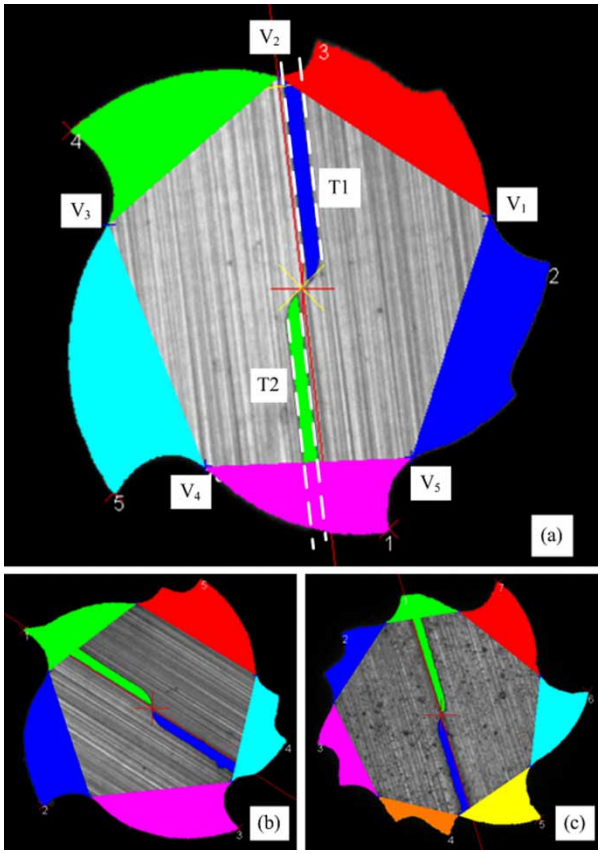

Figure 19. Blade identification and numbering of different fishtail patterns. The blade numbered '1' is identified as the reference blade of the fishtail. Other blades are numbered successively in the counterclockwise direction.

the area, boundary length, and the statistic of the vector angle will be changed. In Figure 20, we illustrate a set of boundary pixels $\{V_s = B_0, B_1, \ldots, B_{m-1}, B_m = V_e\}$ that form a blade starting from V_s and ending at V_e. The definitions of the features of a blade are described below:

- *Area*: It is the area of the object enclosed by the boundary pixels $\{V_s = B_0, B_1, \ldots, B_{m-1}, B_m = V_e\}$ and the line segment $\overline{V_s V_e}$.
- *Boundary length*: It is the number of segments formed by two neighbouring boundary pixels of the blade. It is denoted by 'm'.
- *Statistic of vector angle*: Each boundary pixel has an associated vector angle. The vector angle of B_i is defined as

$$\theta_i = \cos^{-1}\left(\frac{\overrightarrow{B_iB_{i-k}} \cdot \overrightarrow{B_iB_{i+k}}}{\left|\overrightarrow{B_iB_{i-k}}\right|\left|\overrightarrow{B_iB_{i+k}}\right|}\right), \text{where}$$

$$k < i < m - k; k \text{ is a parameter to be determined by the experiment.} \quad (4)$$

The vector angle θ_i defined for every B_i will be non-negative and not greater than 180°, i.e., $0° \leqq \theta_i \leqq 180°$. The vector angles of all boundary pixels of a blade are calculated as a set $\{\theta\}$.

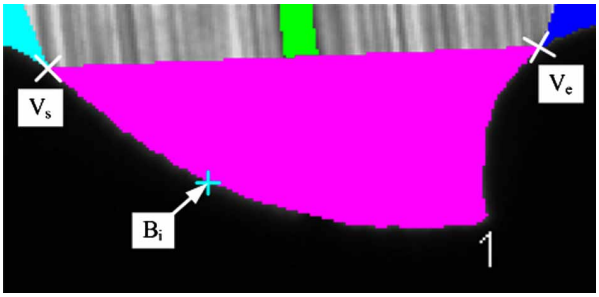

Figure 20. Features of a blade.

The statistic of the vector angle of each blade can be calculated by equation (5). This statistic represents the frequency of the sharp boundary pixels, and the vector angle defined in this way will fall between 45 and 135°

$$S_{\mathrm{VA}} = \left(\left|\{\theta | 45° < \theta < 135°\}\right| / \left|\{\theta\}\right|\right) \times 1000. \tag{5}$$

2.7 Quality control chart

To confirm that the fishtail is not defective, we utilised a training group to set up 'Individuals and Moving Range Chart'. That is, we use the moving range of two successive observations in the set of features of fishtail patterns to measure the process variability [3]. Some routers in a batch are previously identified by experienced inspectors as good training samples. In the training phase, blades with the same number among the training samples are classified into blade sets. Each feature of a blade set is utilised to build one control chart. For instance, since three features of the fishtail with five right flutes are considered, there will be 5 blade sets and 15 quality control charts are constructed. Assume $\{F_i\}$ to be a set of a feature of all the blades with the same blade number in the training group. Then, the UCL and LCL of the control chart can be set by using equations (6)–(11) in the training phase

$$\mathrm{MR}_i = \left|F_i - F_{i-1}\right|, \tag{6}$$

$$\overline{F} = \sum_i F_i / |i|, \tag{7}$$

$$\overline{\mathrm{MR}} = \sum_i \mathrm{MR}_i / |i|, \tag{8}$$

where i is the number of training samples.

$$d_2 = 1.128, \text{ for the sample size is } 2, \tag{9}$$

$$\mathrm{UCL} = \overline{F} + 3 \times \overline{\mathrm{MR}} / d_2, \tag{10}$$

$$\mathrm{LCL} = \overline{F} - 3 \times \overline{\mathrm{MR}} / d_2. \tag{11}$$

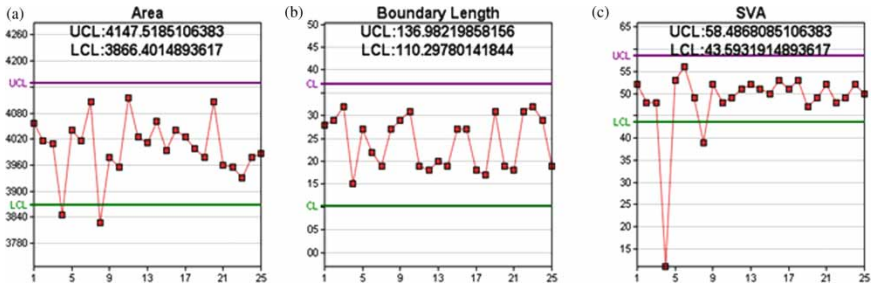

Figure 21. Quality control charts of the defined features of a blade: (a) area, (b) boundary length, and (c) statistic of vector angle.

Figure 21 shows the quality control charts constructed by the above method for each of the defined features. Finally, in the testing phase, when a blade feature is not located between the UCL and LCL, this blade will be classified as collapsed/defective.

3. Experimental results and discussion

In this section, we present some experimental results of fishtail collapse inspection and the performance of the proposed AOI system. Figure 22 shows the prototype of the proposed AOI hardware architecture. Two types of routers with different fishtail patterns are used in the experiment. For each type of fishtail pattern, 25 defect-free routers are used to construct the quality control charts in the training phase. In the testing phase, another 25 inspecting routers are used to verify the accuracy and robustness of the proposed AOI system. It takes less than 3 s to inspect each fishtail.

In Figures 23(a)–(f), we show the details of the inspection process for a fishtail with five blades. Figure 23(a) shows an image captured by the proposed AOI system. Figure 23(b) shows a captured image that is binarised and segmented. Figure 23(c) shows the identified centre of the fishtail. The 1D centroidal profile of the fishtail boundary is shown in Figure 23(d). The blades are segmented from the fishtail, and the reference blade is identified and numbered as '1'. Other blades are numbered successively in the counterclockwise direction as shown in Figure 23(e). Figure 23(f) shows the constructed quality control charts and the details of features and inspection results of the blade. Some of the inspection results obtained by the proposed AOI system, including the area (A), boundary length (BL), and statistic of the vector angle (S_{VA}), of 2 of the 5 blades of 25 sample routers are listed in Table 1. The values indicated

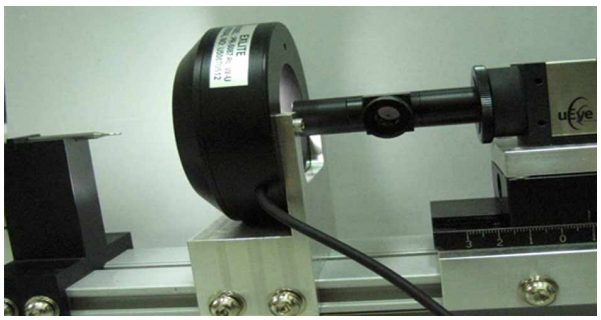

Figure 22. Prototype of the proposed AOI hardware architecture.

(a)

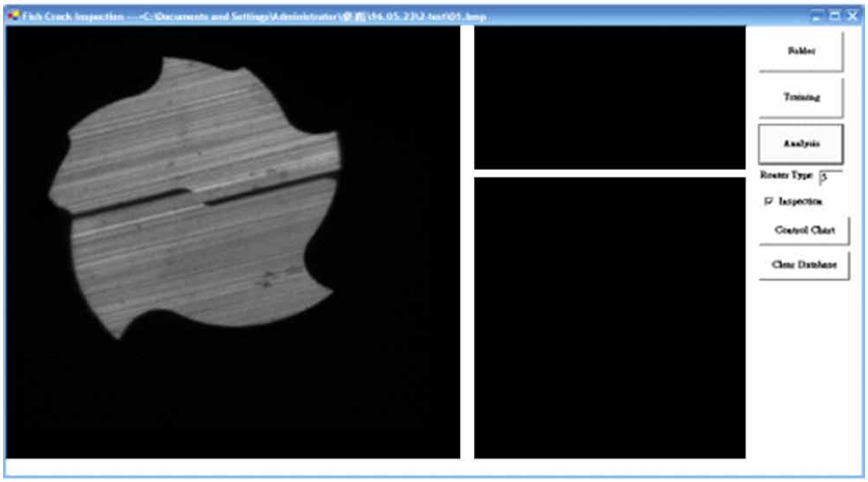

(b)

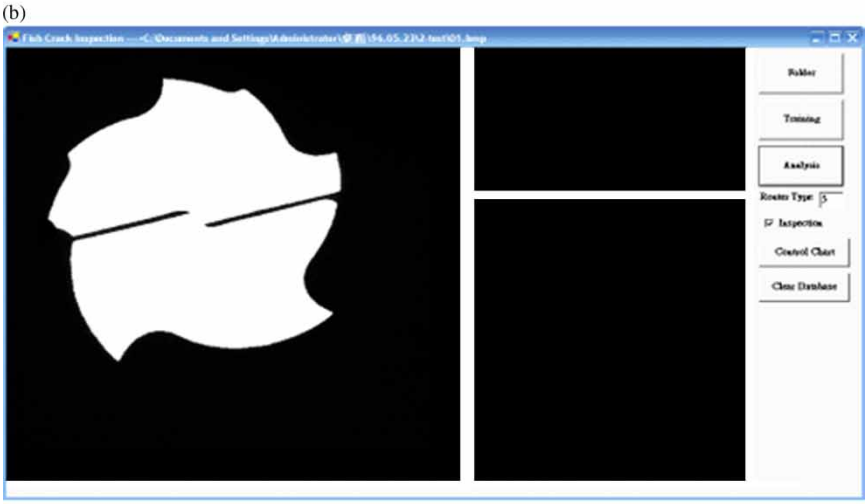

(c)

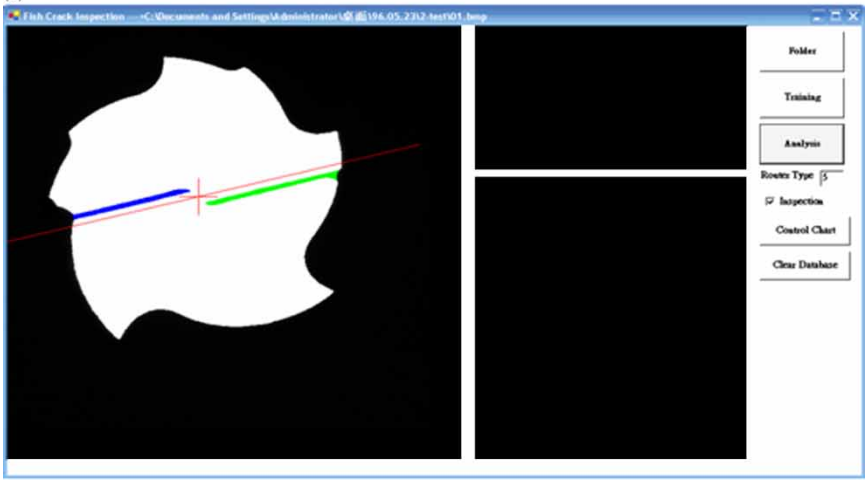

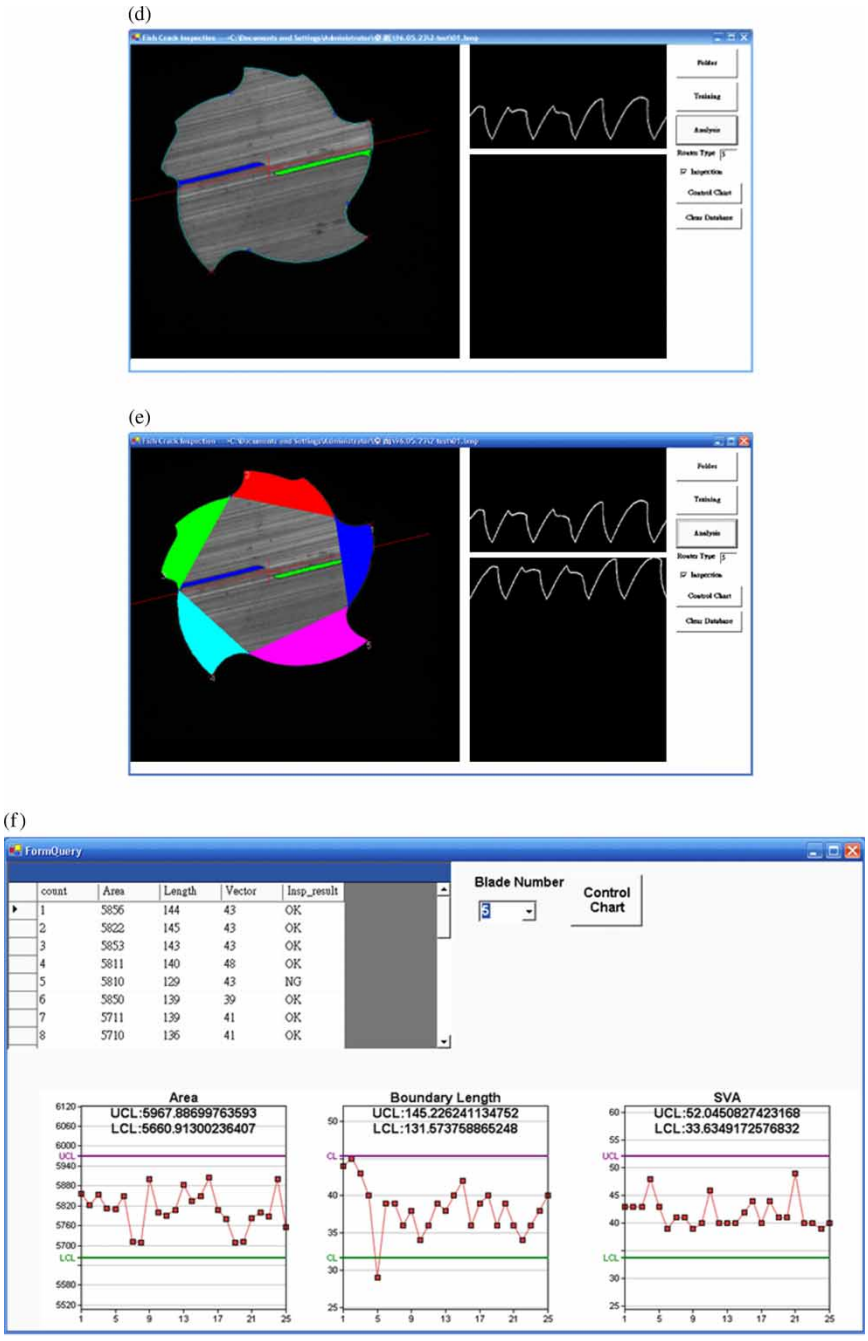

Figure 23. Execution of the proposed AOI system for fishtail collapse inspection: (a) image acquisition, (b) image binarisation, (c) boundary extraction and centre identification, (d) centroidal profile, (e) blade identification, and (f) quality control charts and inspection results.

Table 1. Inspection results of 2 of the 5 blades of the 25 sample routers.

	Blade number								
	1				*2*				*3* ...
Router number	*Area*	*BL*	S_{va}	*R*	*Area*	*BL*	S_{va}	*R*	...
1	4057	128	52	OK	4581	122	69	OK	...
2	4015	129	48	OK	4594	122	69	OK	...
3	4010	132	48	OK	*4541**	*123**	*42**	NG	...
4	*3844**	*115**	*11**	NG	4682	122	62	OK	...
5	4041	127	53	OK	4559	125	76	OK	...
6	4016	122	56	OK	4490	121	70	OK	...
7	4106	119	49	OK	4541	120	69	OK	...
8	*3826**	*127**	*39**	NG	4542	120	65	OK	...
9	3977	129	52	OK	*4389**	*124**	*71**	NG	...
10	3956	131	48	OK	4512*	118*	56*	OK	...
11	4116	119	49	OK	4557	124	68	OK	...
12	4024	118	51	OK	4533	121	70	OK	...
13	4011	120	52	OK	4606	120	78	OK	...
14	4060	119	51	OK	4636	121	64	OK	...
15	3994	127	50	OK	4647	121	68	OK	...
16	4041	127	53	OK	4559	125	76	OK	...
17	4024	118	51	OK	4533	121	70	OK	...
18	3998	117	53	OK	4691	120	64	OK	...
19	3978	131	47	OK	4542	120	65	OK	...
20	4106	119	49	OK	4541	120	69	OK	...
21	3960	118	52	OK	4478	122	69	OK	...
22	3956	131	48	OK	4593	122	62	OK	...
23	3930	132	49	OK	*4521**	*118**	*43**	NG	...
24	3977	129	52	OK	4537	120	69	OK	...
25	3987	119	50	OK	4600	121	64	OK	...
Misdetection rate = 0.008					Successful detection rate = 0.992				
False alarm rate = 0									

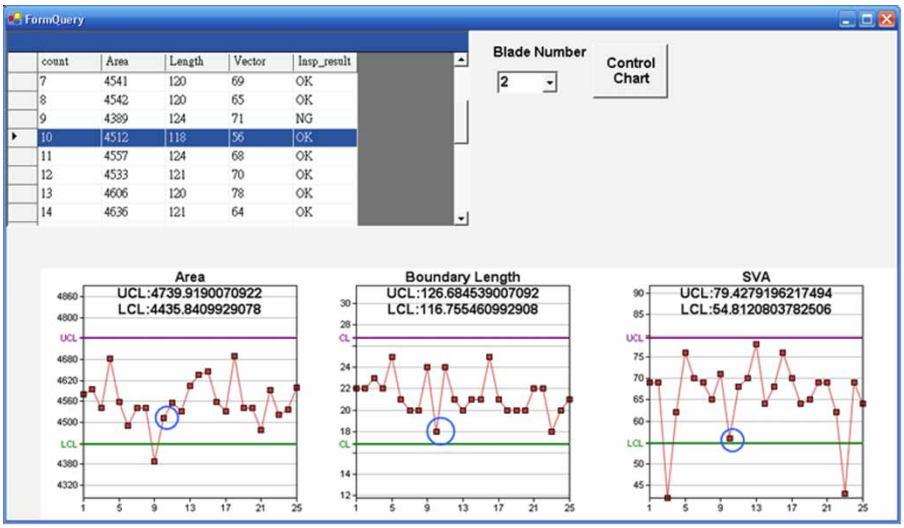

Figure 24. Control chart of blade 2 of router 10.

by the superscript '*' indicate that the collapse in the blade was judged by experienced inspectors. The values in bold type indicate that the collapse in the blade is detected by the proposed AOI system, such as blade 1 of router 4. From the 25 sample routers, 24 routers are detected successfully. The successful detection rate is up to 99.2%.

The proposed AOI system can identify almost all the collapsed blades that can be identified by experienced inspectors, except blade 2 of router 10. In Figure 24, we show the quality control charts constructed according to the extracted features of blade 2 of router 10. The S_{VA} value of this blade is 56, and the associated LCL is 54.8. In this case, the control limit of S_{VA} is set too loose, and the blade will be detected as a good blade. It causes a misdetection. However, if the control limits of S_{VA} are set to tight, some other false alarm might be triggered.

4. Conclusions

In this paper, we have presented an AOI system that can be used to detect and identify the fishtail collapse of routers. The successful detection rate of the proposed AOI system is up to 99.2%. Experimental results show that it is accurate, robust, and easy to use. The merits of the proposed AOI system are as follows: (1) it is the first AOI system proposed for identifying the fishtail collapse of routers; (2) the proposed method is accurate, robust, and suitable for various patterns of fishtails; and (3) the proposed fishtail collapse inspection method is independent of the mounting orientation of the router. However, the proposed AOI system needs some templates to construct a new set of control limits for routers with new fishtail patterns. This will increase the workload. An AOI system with template-free methods could be a future research topic. Moreover, there are some types of routers that require to be coated. The problem of a significant uneven coating that may affect the inspection process has not been discussed here and will be a topic for future study.

Acknowledgements

This work was partly supported by the National Science Council of Taiwan, ROC, under Contract No. NSC 96-2221-E-009-077-MY3. The authors also express their thanks to Cosmos Vacuum Technology Corporation, Taiwan, ROC, for providing the microrouter samples.

References

[1] E.R. Davies, *Machine Vision: Theory, Algorithms, Practicalities*, Academic Press, London, 1990.
[2] L.F. Da-Costa and R.M. Cesar, Jr, *Shape Analysis and Classification: Theory and Practice*, CRC Press, Boca Raton, FL, USA, 2001.
[3] D.C. Montgomery, *Introduction to Statistical Quality Control*, John Wiley & Sons, NJ, USA, 2000.
[4] D.B. Perng, C.Y. Hung, and Y.C. Chen, *An AOI system for microdrill measurement, in Proceedings of the 18th International Conference on Production Research*, Salerno, Italy, 2005.
[5] L.G. Shapiro and G.C. Stockman, *Computer Vision*, Prentice Hall PTR, Englewood Cliffs, Upper Saddle River, NJ, USA, 2001.
[6] F.C. Tien, C.H. Yeh, and K.H. Hsieh, *Automated visual inspection for microdrills in printed circuit board production*, Int. J. Prod. Res. 42 (2004), pp. 2477–2495.